Study of $\nu d \to \mu^- p p_s$ and $\nu d \to \mu^- \Delta^{++}(1232) n_s$ using the BNL 7-foot deuterium-filled bubble chamber

T. Kitagaki, H. Yuta, S. Tanaka, A. Yamaguchi, K. Abe, K. Hasegawa, K. Tamai,* H. Sagawa,* K. Akatsuka,† K. Furuno, and K. Tamae
Tohoku University, Sendai, Japan

M. Higuchi and M. Sato
Tohoku Gakuin University, Sendai, Japan

S. A. Kahn, M. J. Murtagh, R. B. Palmer, N. P. Samios, and M. Tanaka
Brookhaven National Laboratory, Upton, New York 11973
(Received 8 January 1990)

The weak nucleon axial-vector (F_A) and vector (F_V) form factors are determined from the momentum-transfer-squared (Q^2) distributions using 2538 $\mu^- p$ and 1384 $\mu^- \Delta^{++}$ events. The data were obtained from 1 800 000 pictures taken in the BNL 7-foot deuterium-filled bubble chamber exposed to a wide-band neutrino beam with a mean energy $E_\nu = 1.6$ GeV. In the framework of the conventional $V-A$ theory with standard assumptions, the value obtained from the $\mu^- p$ events for the axial-vector mass M_A in the pure dipole parameterization is $1.070^{+0.040}_{-0.045}$ GeV and from the $\mu^- \Delta^{++}$ events is $1.28^{+0.08}_{-0.10}$ GeV. These results are in good agreement with an earlier measurement from this experiment and other recent results. The reaction mechanisms for both processes are compared and found to be very similar. A two-parameter fit for the quasielastic reaction, using dipole forms for F_V and F_A, yields $M_A = 0.97^{+0.14}_{-0.11}$ GeV and $M_V = 0.89^{+0.04}_{-0.07}$ GeV, which is in good agreement with the conserved-vector-current value of $M_V = 0.84$ GeV. Possible deviations from the standard assumptions are also discussed.

I. INTRODUCTION

The weak and electromagnetic structure of the nucleon has been studied both theoretically and experimentally for many years. The vector form factor $F_V(Q^2)$, which has been successfully explored in high-energy elastic electron scattering, is well described by a dipole form factor $\lambda(Q^2)/(1+Q^2/M_V^2)^2$ with a vector mass M_V and a correction factor $\lambda(Q^2)$ to correct for a few-percent deviation from a pure dipole form factor.

The weak nucleon structure has been investigated in several experiments using both quasielastic neutrino scattering $\nu_\mu n \to \mu^- p$,[1-3] and the Δ^{++} production reaction, $\nu_\mu p \to \mu^- \Delta^{++}$.[4-8] Both the vector ($F_V$) and the axial-vector ($F_A$) form factors can be measured using either neutrino quasielastic scattering or Δ^{++} production reaction in deuterium bubble-chamber experiments. The form factor F_A is usually parametrized in terms of the axial-vector mass (M_A) and determined using the $V-A$ theory with the standard assumptions of conserved vector current (CVC), an absence of second-class currents, and time-reversal invariance. While there have been a number of studies of M_A using the $\mu^- p$ reaction from light-liquid bubble chambers, only one other study using $\Delta^{++}(1232)$ production in D_2 has been reported.[7,8]

In this paper the final results of a detailed study of the quasielatic reaction

$$\nu_\mu + d \to \mu^- + p + p_s \tag{1}$$

and the Δ^{++} reaction

$$\nu_\mu + d \to \mu^- + \Delta^{++}(1232) + n_s \ , \tag{2}$$

where p_s and n_s are the spectator proton and neutron respectively, are presented. The data were taken with the 7-foot deuterium-filled bubble chamber exposed to the wide-band neutrino beam at the Alternating Gradient Synchrotron (AGS) at Brookhaven National Laboratory. The primary objective of this study was to determine the axial-vector mass (M_A) using the dipole form of F_A and to compare the mass values obtained from the two reactions. Parametrizations of F_A other than the conventional dipole form are considered and the standard assumptions used in extracting M_A are tested. In the determination of M_A, the effects of the deuteron should be taken into account. Since theoretical calculations for the deuteron effects are only available for reaction (1), caution must be taken in comparing the values of M_A determined from the two processes. The results of a comparison of the two reaction mechanisms are presented. In Sec. II details of the experiment are presented while in Sec. III the procedures used in the form factor analysis are discussed. The results of the various analyses are discussed in Sec. IV and the conclusions from this study are detailed in Sec. V.

II. EXPERIMENTAL PROCEDURE

The data were obtained from a total of 1 800 000 pictures taken in the 7-foot deuterium-filled bubble chamber exposed to a wide-band neutrino beam with a mean energy of 1.6 GeV from the Alternating Gradient Synchrotron at Brookhaven National Laboratory. The final data samples for reactions (1) and (2) are obtained from all exposures of the chamber and the sample for reaction (1) is approximately twice the size of that used in an earlier analysis.[1] Details of the experiment and a full description of the chamber have been given elsewhere.[1]

The film was scanned for neutral-induced interactions with more than one visible charged track. Approximately 32% of the film was rescanned, yielding scanning efficiencies of 0.90±0.01, 0.95±0.01, and 0.93±0.01 for the two-, three-, and all-prong event topologies, respectively. Each event was measured and processed through the geometry program TVGP and the kinematic-fitting program SQUAW, and then examined by physicists.

Neutrino charged-current events were selected by imposing the following requirements: (1) the magnitude of the total visible momentum vector must be greater than 150 MeV/c; (2) the angle between the total visible momentum vector and the neutrino-beam direction must be less than 50°; and (3) at least one of the negative tracks must either leave the chamber without interacting, or stop in a plate with a range consistent with a muon interpretation, or decay into an electron. The initial data set contained approximately 8100 charged-current and 800 neutral-current event candidates inside a restricted fiducial volume of 4 m^3. The candidates for the reactions $\nu_\mu d \to \mu^- pp_s$ and $\nu_\mu d \to \mu^- p\pi^+ n_s$ were selected using three-constraint fitting and particle identification. If the spectator nucleon was not measured, an initial value of 0±45 MeV/c for each component of the spectator momentum (P_x, P_y, P_z) was assigned in the fit. A total of 2684 $\mu^- pp_s$ and 1610 $\mu^- p\pi^+ n_s$ events were obtained with a χ^2 fit probability greater than 1% and with the particle identification consistent with the track mass hypothesis in the successful fit. If an event fit to two reaction hypotheses, the hypothesis with a larger χ^2 probability was accepted. In Table I the data used for the present analysis are summarized.

Events in reaction (1) with low-momentum recoil protons and slow spectator protons would appear in the film as one-prong events and would be lost at the scanning stage. However, it is possible to estimate the effect of this problem on the subsequent analysis. Figure 1(a) shows the spectator proton momentum distribution for reaction (1). The shaded region in this figure denotes measured spectator protons where the spectator is defined to be the slower of the two measured protons. The unshaded area corresponds to the two-prong events in which the momenta for the invisible spectator protons are obtained from the kinematic fit. The curve represents the prediction from the Hulthén wave function and it describes the data adequately except for $P_s > 200$ MeV/c, where the rescattering effects in deuterium become apparent. The

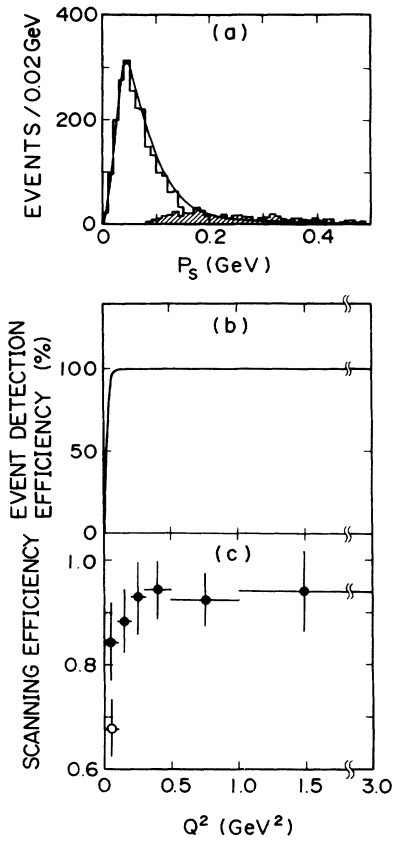

FIG. 1. (a) The spectator-proton momentum distribution with the prediction from the Hulthén wave function. The shaded and the unshaded areas correspond to the measured and the fitted spectator momenta for quasielastic $\nu_\mu d \to \mu^- pp_s$ events. (b) The event detection efficiency as a function of Q^2. (c) The average scanning efficiencies with the event detection efficiency (solid circle) and without the event detection efficiency (open circle).

TABLE I. Summary of events.

Reaction	Observed	$0.5 < E_\nu < 6.0$ GeV	$Q^2 < 3.0$ GeV^2 ($0.1 < Q^2 < 3.0$ GeV^2)
$\nu d \to \mu^- pp_s$	2684	2544	2538 (2310)
$\nu d \to \mu^- p\pi^+ n_s$	1610	1547	
$1.08 < M(\pi p) \leq 1.40$ GeV		1385	1384 (1232)

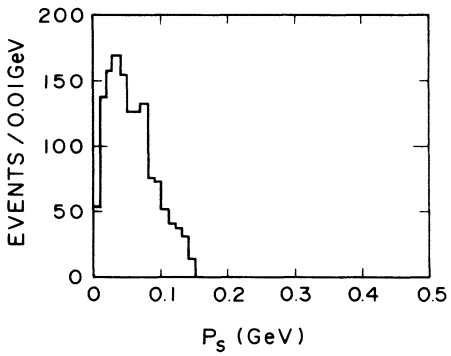

FIG. 2. The fitted spectator-neutron momentum distribution for the Δ^{++} events.

proton detection efficiency is then the ratio of observed spectators to predicted spectators from the distribution of Fig. 1(a), where one assumes that the proton detection for $P_s > 200$ MeV/c is 100%. Using this proton detection together with Monte Carlo–generated events for reaction (1), it is possible to calculate an event detection probability (i.e., ≥ 2 prongs visible on the scanning table) as a function of Q^2. The resulting curve shown in Fig. 1(b) indicates, as expected, that the losses due to missing 1-prong events are at very low Q^2 and for values of $Q^2 \geq 0.08$ (GeV/c)^2 no correction is required. The effect of the loss of 1-prong events on the scanning efficiency as a function Q^2 is clearly visible in Fig. 1(c). In addition to these experimental problems, the low-Q^2 region is also most sensitive to nuclear corrections and to Fermi motion corrections. Consequently, in the maximum-likelihood analysis of the Q^2 distribution to determine the form factors, only the region $Q^2 \geq 0.10$ (GeV/c)^2 is used.

A potentially important experimental problem for the study of the Δ^{++} reaction is that the spectator neutron is not measurable. Since the kinematic fitting procedure constrains spectators to relatively low momenta, this implies a cutoff in the neutron spectator momentum. This can be seen by comparing the neutron-spectator momentum distribution (Fig. 2) for the Δ^{++} reaction with the previously discussed proton-spectator momentum distribution [Fig. 1(a)] for the quasielastic scattering where the measured high-energy tail is apparent. One way to assess the impact of this limitation is to consider the sensitivity of the quasielastic results to a cut on the spectator-proton momentum. As is discussed below there is no evidence of a significant change in the value of M_A determined from the quasielastic scattering if only events with $P_s < 50$ MeV/c are used. Consequently, one might not expect the Δ^{++} reaction results to be sensitive to the loss of high-momentum spectators.

The number of selected quasielatic events in the neutrino energy range $0.5 \leq E_\nu \leq 6.0$ GeV and $0.1 \leq Q^2 \leq 3.0$ (GeV/c)^2 is 2310. The primary background comes from the reaction $\nu_\mu d \to \mu^- p \pi^0 p_s$. This background was estimated to be $\sim 5\%$ using three-constraint fit $\nu_\mu d \to \mu^- p \pi^+ n_s$ events. The overall correction factor was found to be 1.11 ± 0.04 including the one-prong correction of 2.3% estimated from the event detection efficiency shown in Fig. 1(b). Table II(a) details the corrections for the $\nu_\mu d \to \mu^- pp_s$ reaction. It should be noted that these corrections only affect the total number of quasielastics in the data and they do not affect the shape of the Q^2 distribution in the region of interest.

Figure 3 shows the $p\pi^+$-mass [$M(p\pi^+)$] distribution for the $\mu^- p \pi^+$ state. The curve is the result of the best fit to the distribution using a relativistic Breit-Wigner res-

TABLE II. Corrections for the $\nu d \to \mu^- pp_s$ and $\nu d \to \mu^- p \pi^+ n_s$ reactions.

Correction		Correction factor
(a) $\nu d \to \mu^- pp_s$		
Scanning efficiency	g_1	1.092±0.025
Measuring efficiency	g_2	1.038±0.030
One-prong correction	g_3	1.023
χ^2 proability cut	g_4	1.010
Background		
$\nu d \to \mu^- p \pi^0 p_s$	g_5	0.948±0.008
$\nu d \to \nu p \pi^- p_s$	g_6	0.998±0.001
Total correction	$g_1 \times g_2 \times g_3 \times g_4 \times g_5 \times g_6$	1.110±0.040
(b) $\nu d \to \mu^- p \pi^+ n_s$		
Scanning efficiency	g_1	1.092±0.037
Measuring efficience	g_2	1.038±0.040
χ^2 probability cut	g_3	1.010
H_2 contamination in D_2	g_4	0.870±0.020
Loss of fast neutron spectator	g_5	1.220±0.010
Background		
$\nu d \to \mu^- p \pi^+ \pi^0 n_s$	g_6	0.977±0.008
$\nu d \to \nu p \pi^+ \pi^- n_s$	g_7	0.998±0.001
Total correction	$g_1 \times g_2 \times g_3 \times g_4 \times g_5 \times g_6 \times g_7$	1.123±0.059

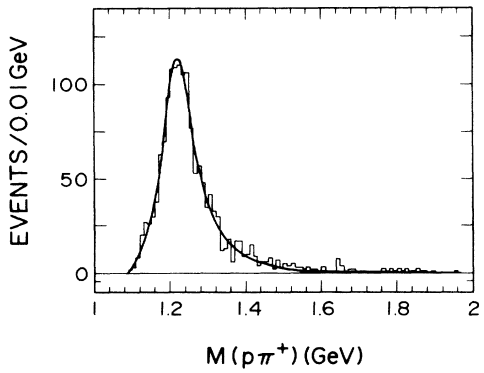

FIG. 3. The effective-mass distribution for the $\mu^- p\pi^+ n_s$ events.

onance form with a three-body phase-space background. The phase-space component obtained from the fit was less than 1%.[4] The number of selected $\mu^-\Delta^{++}$ events with the $p\pi^+$ mass of $1.08 \le M(p\pi^+) \le 1.40$ GeV, neutron energy $0.5 \le E_\nu \le 6.0$ GeV and $0.1 \le Q^2 \le 3.0$ $(\mathrm{GeV}/c)^2$ is 1232. The primary background comes from the reactions $\nu_\mu d \to \mu^- p\pi^+ n_s \pi^0$ and $\nu_\mu d \to \nu_\mu p\pi^+\pi^- n_s$ and from a $(13\pm2)\%$ H_2 contamination in the deuterium.[1] There is also a systematic event loss from the kinematic fitting due to fast neutron spectators and the scanning-measuring inefficiency. The overall correction factor was estimated to be 1.123 ± 0.059 and is described in detail in Ref. 4. Table II(b) lists the corrections for the $\nu d \to \mu^- p\pi^+ n_s$ reaction. Again, these corrections do not affect the Q^2 distribution in the region of interest.

Figures 4(a) and 4(b) show the neutrino-energy (E_ν) distributions for the quasielastic and Δ^{++} production reactions. Both distributions peak at approximately 1.2 GeV. Figures 5(a) and 5(b) show the momentum-transfer-squared (Q^2) distributions for reactions (1) and (2). The scanning and measuring efficiencies are included in these distributions as well as the correction for the one-prong event loss for reaction (1) shown in Fig. 1(b). The curves in Fig. 5 are the theoretical predictions which will be discussed in Sec. IV.

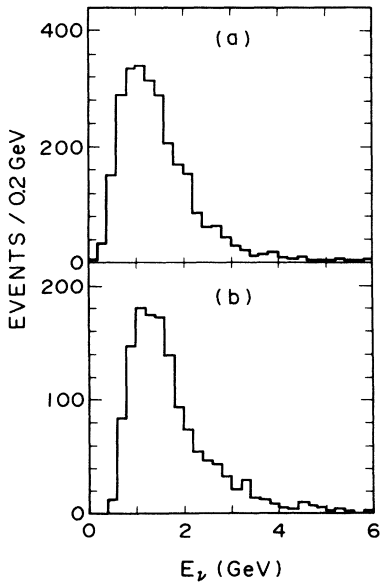

FIG. 4. The E_ν distribution for (a) the quasielastic and (b) the Δ^{++} production reactions.

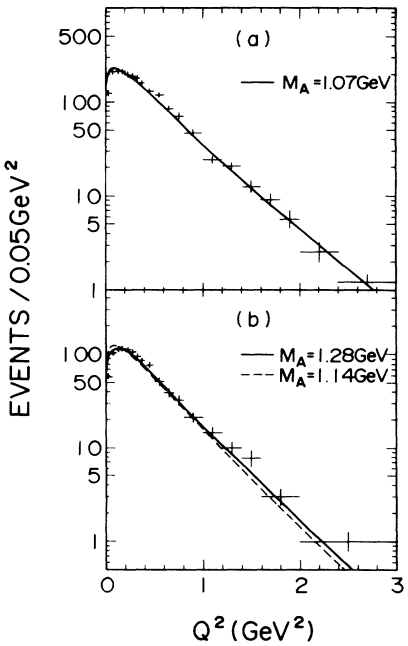

FIG. 5. The Q^2 distribution for (a) the quasielastic and (b) the Δ^{++} production reactions. The curves are the theoretical predictions obtained from least-squares fits with the fitted M_A values for the $Q^2 < 3.0$ $(\mathrm{GeV}/c)^2$.

III. FORM-FACTOR ANALYSIS

To extract the weak nucleon form factors from reactions (1) and (2), the experimental data are fit to the theoretical predictions using maximum-likelihood method. Denoting the hadronic mass $M(p\pi^+)$ as W, the predictions of the cross sections, $d\sigma/dQ^2$ and $d^2\sigma/dQ^2W^2$, are formulated from the standard $V-A$ theory with the following assumptions: (i) time-reversal invariance and charge symmetry, (ii) partial conservation of vector-current, and (iii) conservation of vector current (CVC). The vector form factor $F_V(Q^2)$ is taken to be the dipole form $F_V(Q^2) = \lambda(Q^2)/(1+Q^2/M_V^2)^2$ where $M_V = 0.84$ GeV,[9] and $\lambda(Q^2)$ is a correction factor accounting for small deviations from a pure dipole form obtained from electron scattering data.[10] Under these assumptions, the axial-vector form factor is the only unknown. A complete description of the cross sections may be found elsewhere.[11,12]

In quasielastic scattering, the axial-vector form factor $F_A(Q^2)$ is conventionally parametrized by a dipole form:

$$F_A(Q^2) = -1.254/(1+Q^2/M_A^2)^2 , \quad (3)$$

where M_A is the axial-vector mass. The maximum-likelihood function L^Q used in this analysis is given by

$$L^Q(M_A)=\prod_{i=1}^{N}\left[\frac{R(Q_i^2)d\sigma/dQ_i^2}{\int_{Q^2_{\min}}^{Q^2_{\max}} R(Q^2)(d\sigma/dQ^2)dQ^2}\right]^{\omega(Q_i^2)}, \tag{4}$$

where N is the total number of events in the Q^2 range from $Q^2_{\min}$ to $Q^2_{\max}$, $R(Q_i^2)$ is the correction factor[13] for the free-neutron cross section due to the effects of the Pauli exclusion principle and deuteron binding and $\omega(Q_i^2)$ is an event weight based on the scanning efficiency.

There are several theoretical models[12,14–17] for Δ^{++} production which are based on the hypotheses outlined above. Detailed comparisons[8,17] of these predictions to other experimental data have shown that the Adler model[12] best describes the data. In this analysis the Adler model as developed by Schreiner *et al.*[17] is used. The axial-vector form factors are parametrized as

$$F_i^A(Q^2)=\frac{c_i(0)[1+\alpha_i Q^2/(b_i+Q^2)]}{(1+Q^2/M_A^2)^2} \quad (i=3,4,5), \tag{5}$$

where $c_i(0)$, a_i, b_i are the model-dependent axial-vector form-factor parameters determined for the Adler model:[17]

$$c_3(0)=0, \quad c_4(0)=-0.3, \quad c_5(0)=1.2,$$

$$a_3=b_3=0, \quad a_4=a_5=-1.21, \quad b_4=b_5=2.0.$$

The likelihood function L^D in this case is defined as

$$L^D(M_A)=\prod_{i=1}^{N}\left[\frac{d^2\sigma/dQ_i^2dW_i^2}{\int_{Q^2_{\min}}^{Q^2_{\max}}\int_{W^2_{\min}}^{W^2_{\max}}(d^2\sigma/dQ^2dW^2)dQ^2dW^2}\right]^{\omega(Q_i^2)}, \tag{6}$$

where $W_{\min}$ and $W_{\max}$ are taken to be 1.08 and 1.4 GeV, respectively. To compare the M_A values from reactions (1) and (2), we have used events with $0.1 \le Q^2 \le 3.0$ $(\mathrm{GeV}/c)^2$ for both reactions. Maximum-likelihood fits to the data with the dipole axial-vector form factors have been performed for reactions (1) and (2), and the results are given in the next section.

IV. RESULTS

A. The quasielastic reaction $\nu_\mu d \to \mu^- pp_s$

With the standard assumptions and $M_V=0.84$ GeV, a one-parameter fit to the data yields

$$M_A=1.070^{+0.040}_{-0.045}\ \mathrm{GeV} \tag{7}$$

for the dipole form in the Q^2 range $0.1 \le Q^2 \le 3.0$ $(\mathrm{GeV}/c)^2$. This value is more than 4 standard deviations from the equality $M_A=M_V=0.84$ GeV. The curve in Fig. 5(a) is the prediction with $M_A=1.07$ GeV fitted to the distribution for $Q^2<3.0$ $(\mathrm{GeV}/c)^2$. There is a good agreement with the data for all Q^2.

Since there is no theoretical basis for the assumption of a dipole form, we have also fit to a quark model with axial-vector-meson dominance (QM-AVMD) suggested by Sehgal:[18]

$$F_A(Q^2)=F_A(0)(1+Q^2/M_A^2)^{-1} \times \exp[-\tfrac{1}{6}Q^2R^2/(1+Q^2/4M_p^2)], \tag{8}$$

where $R^2=6\ \mathrm{GeV}^{-2}$ and M_p is the proton mass. The result of the fit is $M_A=1.37\pm0.13$ GeV for QM-AVMD. It is interesting to note that this value is consistent with the mass of the $a_1(1260)$ meson[19] with a full width of 330 MeV, though the mass value is quite sensitive to the form used for $F_A(Q^2)$.

A simple monopole form for $F_A(Q^2)$ is excluded at the level of 5 standard deviations based on the likelihood-function analysis.

By fitting both M_A and M_V simultaneously to dipole forms, one can test the CVC prediction of $M_V=0.84$ GeV. Figure 6 shows the one-standard-deviation contour plot of L^Q in (M_V,M_A) space. This fit yields $M_A=0.97^{+0.14}_{-0.11}$ GeV and $M_V=0.89^{+0.04}_{-0.07}$ GeV, in agreement with the value of $M_V=0.84$ GeV.[10]

The present results are consistent with a previous result of this experiment[1] as well as the results from other experiments.[2,3] These various results are summarized in Table III for the single-parameter fits and in Table IV for the two-parameter fits. All the errors quoted correspond to a change in the corresponding likelihood functions by 0.5 units.

In this analysis the deuterium-target effects are taken into account by applying the correction factor[13] $R(Q^2)$

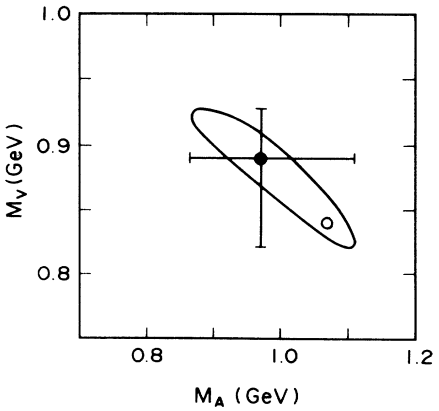

FIG. 6. The one-standard-deviation contour plot of L^Q in (M_V,M_A) space. The open circle is the point obtained from the one parameter fit.

TABLE III. Axial-vector mass M_A in the dipole form factor from $\nu+H_2/D_2$ experiments.

E_ν (GeV)	Raw events	M_A (GeV)	Reference
		(a) $\nu+n\to\mu^- p$	
0.5–6.0	2544	$1.070^{+0.040}_{-0.045}$	This expt.
0.3–6.0	1138	1.07±0.05	This expt., BNL 1981 (Ref. 1)
0.15–3.0	1737	1.00±0.05	ANL 1982 (Ref. 2)
5.0–200	362	$1.05^{+0.12}_{-0.16}$	Fermilab 1983 (Ref. 3)
		(b) $\nu+p\to\mu^-\Delta^{++}$	
0.5–6.0	1385	$1.28^{+0.08}_{-0.10}$	This expt.
0.5–6.0	672	1.14±0.014	This expt. ($P_s<50$ MeV)
5.0–100	138	1.25±0.15	Fermilab 1978 (Ref. 5)
5.0–200	551	0.85±0.10	BEBC 1980 (Ref. 6)
0.5–6.0	871	0.98±0.06	ANL 1982 (Refs. 7,8)

for the free-neutron cross section, which is calculated using the impulse approximation with the Hulthén wave function for the deuteron. A number of other theoretical calculations of these deuteron effects have been made using various deuteron wave functions with and without final-state interactions, or using different methods such as the closure approximation or the elementary-particle-model approach.[20,21] The numerical results are all comparable and they all indicate that the deuteron effects are important only for $Q^2<0.1$ (GeV/c)^2.

To investigate a possible deviation from the pure dipole form factor, the M_A values from the maximization of the likelihood function are plotted as a function of the $Q^2_{\min}$ cut in Fig. 7(a). The arrow in Fig. 7(a) indicates the lower limit $Q^2_{\min}=0.1$ (GeV/c)^2 used to obtain the value $M_A=1.07$ GeV (the dashed line). For $Q^2_{\min}\geq 0.06$ (GeV/c)^2 the value of M_A obtained is insensitive to the actual $Q^2_{\min}$ used. However for lower $Q^2_{\min}$ there is an indication of a change in the M_A obtained. This may in large part be due simply to the difficulty of correction for losses in low-Q^2 (single-prong) events or it could reflect problems in correcting for deuteron effects.

The effects of the deuteron binding are known to be very strong at $Q^2\simeq 0$ and they reduce the deuteron cross section by 40%. To study this effect further, Fig. 7(b) shows the M_A distribution as a function of the $Q^2_{\min}$ cut for events with spectator-proton momentum $P_s<50$ MeV/c. Events with low P_s are likely to be less affected by the deuteron effects. Again there is an indication that the M_A value rises for very low $Q^2_{\min}$ cuts. However, the likelihood fit for events with $P_s<50$ MeV yields $M_A=1.07\pm0.07$ GeV for $Q^2_{\min}=0.1$ (GeV/c)^2. This is identical to the value of M_A obtained for all the events irrespective of their spectator momentum. These studies suggest that for $Q^2_{\min}\geq 0.1$ (GeV/c)^2 the deuteron corrections are small and adequate and also that the results obtained are not sensitive to the spectator momentum distribution.

TABLE IV. Axial-vector mass M_A and vector mass M_V from the two-parameter fit for reaction $\nu+n\to\mu^- p$.

M_A	M_V	Reference
$0.97^{+0.14}_{-0.11}$	$0.89^{+0.04}_{-0.07}$	This expt.
1.04±0.14	0.86±0.07	This expt., BNL 1981 (Ref. 1)
0.80±0.10	0.96±0.04	ANL 1982 (Ref. 2)
$0.72^{+0.32}_{-0.20}$	0.90±0.05	Fermilab 1983 (Ref. 3)

B. The reaction $\nu_\mu d\to\mu^-\Delta^{++}n_s$

Using the dipole axial-vector form factors given in Eq. (5) and the likelihood function L^D defined in Eq. (6), a maximum-likelihood fit was performed for the 1232 $\mu^-\Delta^{++}$ events with $0.1\leq Q^2\leq 3.0$ (GeV/c)^2. Since the correction $R(Q^2)$ for quasielastic scattering is only significant in the small-Q^2 region [$Q^2<0.1$ (GeV/c)^2], only the Q^2 region from 0.1 to 3 (GeV/c)^2 is used for the

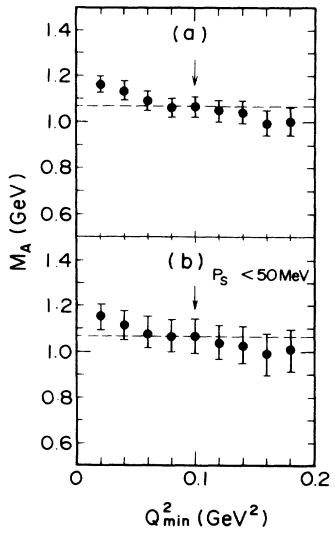

FIG. 7. The axial-vector mass M_A as a function of $Q^2_{\min}$ for the quasielastic events (a) without P_s cut and, (b) with $P_s<50$ MeV/c. The dashed lines correspond to $M_A=1.07$ GeV.

fit in reaction (2). The likelihood fit to the data yields

$$M_A = 1.28^{+0.08}_{-0.10}\ \text{GeV} . \quad (9)$$

This result is more than one standard deviation larger than that obtained from reaction (1). The axial-vector meson mass M_A is expected to be the same for both reactions (1) and (2).

Figure 8(a) shows the dependence of the fitted M_A on the $Q^2_{\min}$ cut. As was true in the case of the quasielastic process, the value of M_A is stable for values of $Q^2_{\min} \geq 0.06$ (GeV/c)^2 and there is an indication of an increase in M_A if a lower $Q^2_{\min}$ is used. As was pointed out earlier the kinematic fitting procedure restricts the spectator neutrons to relatively low momentum. This can clearly be seen by comparing the spectator neutron distribution in Fig. 2 with the corresponding spectator-proton distribution for the quasielastic channel [Fig. 1(a)], where the high-energy tail from the measured spectator proton is significant. In the quasielastic analysis there was no evidence that the value to M_A was sensitive to the momentum range of spectator momenta. A maximum-likelihood analysis using only the Δ^{++} events with $P_s(n) < 50$ MeV/c in the Q^2 range $0.1 \leq Q^2 \leq 3.0$ (GeV/c)^2 yields $M_A = 1.14 \pm 0.14$ GeV. This value is lower but consistent with the fit using all the Δ^{++} events. The $Q^2_{\min}$ dependence of M_A for the events with $P_s(n) \leq 50$ MeV/c is shown in Fig. 8(b). Again the values are consistent for $Q^2_{\min} \geq 0.06$ (GeV/c)^2 but the mean does tend to be lower than in the case when all events are used.

The curves in Fig. 5(b) are the theoretical predictions with $M_A = 1.28$ GeV (solid) and $M_A = 1.14$ GeV (dashed) obtained from the least-squared fit to the data for $Q^2 < 3.0$ (GeV/c)^2. Good agreement is observed between that data and the predictions for $Q^2 \geq 0.2$ (GeV/c)^2. The difference between the two curves becomes larger for higher Q^2 and amounts to $\approx 15\%$ at $Q^2 = 2$ (GeV/c)^2, but the difference is not statistically significant.

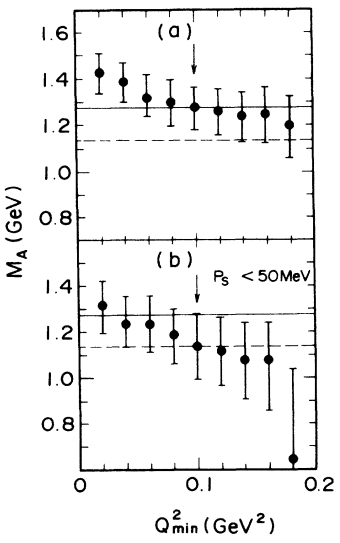

FIG. 8. The axial-vector mass m_A as a function of $Q^2_{\min}$ for the Δ^{++} events (a) without P_s cut, and (b) with $P_s < 50$ MeV/c. The solid and dashed lines correspond to $M_A = 1.28$ and $M_A = 1.14$ GeV, respectively.

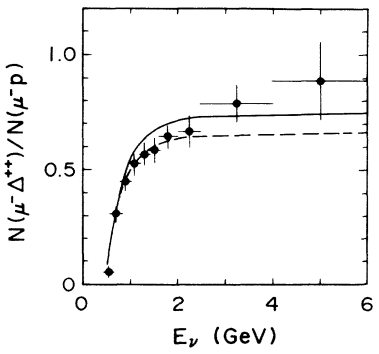

FIG. 9. The E_ν distribution for the ratio of $N(\mu^-\Delta^{++})/N(\mu^- p)$. The curves are the ratios of the corresponding predictions with $M_A = 1.28$ GeV (solid) and $M_A = 1.14$ GeV (dashed) for the Δ^{++} reaction.

C. Comparison of the $\mu^- p$ and $\mu^-\Delta^{++}$ channels

In the naive quark picture the quasielastic and Δ^{++} production reactions are similar to each other. By denoting W^+, u, and d as the positively charged weak boson and the up and down quarks, respectively, these processes are $W^+ + d \to u$ and $u + (du) \to p$ for the $\mu^- p$ reaction, and $W^+ + d \to u$ and $u + (uu) \to \Delta^{++}$ for the Δ^{++} production reaction. The only difference between the quasielastic and the Δ^{++} production reactions is the recombination of the recoiled u quark with different diquark states, resulting in different spin and isospin final states.

To compare these two reactions, the ratios of the 2544 quasielastic events and the 1385 Δ^{++} events with the corrections listed in Table II are used. Figure 9 shows the E_ν distribution of the ratio $N(\mu^-\Delta^{++})/N(\mu^- p)$ where N stands for the number of events. The curves are the ratios of the corresponding predictions with $M_A = 1.28$ GeV (solid) and $M_A = 1.14$ GeV (dashed) for the Δ^{++} reaction and $M_A = 1.07$ GeV for the quasielastic reactions, respectively. The dashed curve with $M_A = 1.14$

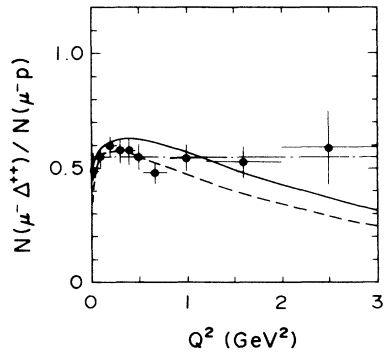

FIG. 10. The Q^2 distribution for the ratio of $N(\mu^-\Delta^{++})/N(\mu^- p)$. The solid and dashed curves correspond to the same ratios as stated in Fig. 9.

GeV describes the data well except for the points with $E_\nu > 2.3$ GeV where the data points lie above the curve by slightly more than one standard deviation. The solid curve with $M_A = 1.28$ GeV does not describe the data as well.

Figure 10 shows the Q^2 distribution of the ratio $N(\mu^- \Delta^{++})/N(\mu^- p)$. The solid and dashed curves correspond to the same ratios as described in Fig. 9. The dashed-dotted line is the average ratio of 0.55. Again, the dashed curve describes the data well compared to the solid curve for $Q^2 < 0.8$ (GeV/c)^2, but deviations became apparent for $Q^2 > 0.8$ (GeV/c)^2. The dashed-dotted line generally describes the data well for the whole range of Q^2. The χ^2 values per degree of freedom are 0.59, 1.12, and 1.61 for the dashed-dotted, dashed, and solid lines, respectively. These results slightly favor the constant ratio which suggests that the Q^2 dependence for the Δ^{++} production reaction is similar to the neutrino quasielastic reaction in spite of the different hadronic spin and isospin final states.

V. CONCLUSION

The quasielastic reaction $\nu_\mu n \to \mu^- p$ and the Δ^{++} production reaction $\nu_\mu p \to \mu^- \Delta^{++}$ have been investigated to study the weak nucleon structure. For the quasielastic reaction, the conventional form-factor analysis yielded the axial-vector mass $M_A = 1.070^{+0.040}_{-0.045}$ GeV for the dipole form and M(QM-AVMD)$= 1.37 \pm 0.13$ GeV for the quark model with axial-vector-meson dominance. Using dipole form factors, a two-parameter fit gave $M_A = 0.97^{+0.14}_{-0.11}$ GeV and $M_V = 0.89^{+0.04}_{-0.07}$ GeV, in good agreement with the CVC hypothesis. These results are in agreement with other recent neutrino results. A dipole axial-vector form factor $F_A(Q^2)$ adequately describes the data in the fitted region $[0.1 \le Q^2 \le 3.0$ (GeV/c)$^2]$. While there is some evidence that the fit is not adequate in the lower-Q^2 region it is unclear, given the experimental uncertainties in this region, if this deviation is significant.

A likelihood fit to the Δ^{++} channel yields $M_A = 1.28^{+0.08}_{-0.10}$ GeV which is consistent with, but a little over 1.5 standard deviations, higher than the value of M_A determined from the quasielastic reaction. In this Δ^{++} analysis no deuteron corrections were applied and the kinematic fitting could not accommodate fast neutron spectators. While the conclusions from the quasielastic analysis are that the analysis is not sensitive to either of these restrictions for the Q^2 and E_ν ranges used the value of M_A from the Δ^{++} analysis does drop to $M_A = 1.14 \pm 0.14$ GeV if only events with very slow spectators are used.

Finally, a comparison of the quasielastic and Δ^{++} production reactions indicates very similar Q^2 and E_ν behavior. In both cases the theoretical ratio using $M_A = 1.14$ GeV from the Δ^{++} reaction is preferred. However, the results of the χ^2 fits for the Q^2 dependence favor constant ratio, suggesting a similar Q^2 dependence for the quasielastic and Δ^{++} production reactions in spite of the different hadronic spin and isospin final states.

ACKNOWLEDGMENTS

We are grateful to the AGS staff, the operation crew of the BNL 7-foot bubble chamber, F. M. Simes who helped in the data processing, and to the scanning and measuring personnel at BNL, Tohoku University, and Tohoku Gakuin University for their dedicated work. This research was supported by the U.S.-Japan Cooperative Program in High Energy Physics under the Japanese Ministry of Education, Science, and Culture and the U.S. Department of Energy under Contract No. DE-AC02-76CH00016.

*Present address: KEK, Ibaraki, Japan.
†Present address: Fujitsu Company, Tokyo, Japan.

[1]N. J. Baker *et al.*, Phys. Rev. D **23**, 2499 (1981).
[2]K. L. Miller *et al.*, Phys. Rev. D **26**, 537 (1982).
[3]T. Kitagaki *et al.*, Phys. Rev. D **28**, 436 (1983).
[4]T. Kitagaki *et al.*, Phys. Rev. D **34**, 2554 (1986).
[5]J. Bell *et al.*, Phys. Rev. Lett. **41**, 1008 (1978).
[6]P. Allen *et al.*, Nucl. Phys. **B176**, 269 (1980).
[7]G. M. Radecky *et al.*, Phys. Rev. D **25**, 1161 (1982).
[8]S. J. Barrish *et al.*, Phys. Rev. D **19**, 2521 (1979).
[9]B. Bartoli *et al.*, Riv. Nuovo Cimento **2**, 241 (1972).
[10]M. G. Olsson *et al.*, Phys. Rev. D **17**, 2938 (1978).
[11]C. N. Llewelyn Smith, Phys. Rep. C **3**, 261 (1971).
[12]S. L. Adler, Ann. Phys. (N.Y.) **50**, 189 (1968); Phys. Rev. D **12**, 2644 (1975).
[13]S. K. Singh, Nucl. Phys. **B36**, 419 (1971).
[14]P. Zucker, Phys. Rev. D **4**, 3350 (1971).
[15]P. Salin, Nuovo Cimento A **48**, 506 (1967).
[16]J. Bijtebier, Nucl. Phys. **B21**, 158 (1970).
[17]P. A. Schreiner and F. Von Hippel, Nucl. Phys. **B58**, 333 (1973); Phys. Rev. Lett. **30**, 339 (1973).
[18]L. Sehgal, in *Proceedings of the European Physical Society International Conference on High Energy Physics*, Geneva, Switzerland, 1979, edited by A. Zichichi (CERN, Geneva, 1980), p. 98.
[19]Particle Data Group, G. P. Yost *et al.*, Phys. Lett. B **204**, 284 (1988).
[20]S. K. Singh and H. Arenhovel, Z. Phys. A **324**, 347 (1986).
[21]S. L. Mintz, Phys. Rev. D **13**, 639 (1976).